Int Ophthalmol (2022) 42:1381–1389
https://doi.org/10.1007/s10792-021-02126-z

ORIGINAL PAPER

Three-dimensional topographic changes of anterior chamber depth following phacoemulsification with intraocular lens implantation in cataract patients

Yuexin Wang · Siman Sun · Shanshan Wei · Yining Guo · Tingyi Wu · Xuemin Li

Received: 3 March 2021 / Accepted: 12 November 2021 / Published online: 5 January 2022

Abstract

Purpose To investigate the three-dimensional topographic changes of anterior chamber depth (ACD) following cataract surgery.

Methods Seventy-eight eyes with age-related cataract undergoing phacoemulsification and intraocular lens (IOL) implantation were retrospectively enrolled. Participants were evaluated with Pentacam for ACD topography before and approximately four weeks after the surgery. The absolute changes of ACD (AACD) and the relative changes of ACD (RACD) topography were calculated, and three-dimensional topographic contours were plotted. The influence of age, gender, distance to corneal apex (DCA), temporal–nasal and superior–inferior on AACD and RACD was analyzed.

Results Both AACD and RACD were negatively correlated with the DCA ($p < 0.001$; $p < 0.001$) and positively correlated with the age at all DCA ($p < 0.05$ for all the analyses). Significantly greater AACD and RACD were observed in female subjects ($p < 0.05$, respectively, at all DCA). AACD was significantly larger in the temporal compared with the nasal region ($p < 0.001$) and at the superior compared with the inferior region ($p < 0.001$), but not RACD. Subgroup analysis indicated that the significant difference of the AACD between the temporal and nasal regions was manifested at the DCA of more than 6 mm ($p < 0.001$), and the difference between the superior and inferior regions was observed at 2 mm DCA for both AACD ($p < 0.001$) and RACD ($p = 0.001$).

Conclusions We depicted the topographic changes of ACD following cataract surgery and found that it was significantly influenced by age, gender, DCA and quadrant location. The research provided the basis for including postoperative ACD topography prediction before cataract surgery in the future.

Keywords Topography · Anterior chamber depth · Cataract surgery · Intraocular lens

Yuexin Wang and Siman Sun contributed equally to this work.

Y. Wang · S. Sun · S. Wei · Y. Guo · T. Wu · X. Li (✉)
Beijing Key Laboratory of Restoration of Damaged Ocular Nerve, Department of Ophthalmology, Peking University Third Hospital, 49 North Garden Road, Haidian District, Beijing 100191, China
e-mail: 13911254862@163.com

Y. Wang · S. Sun · S. Wei · Y. Guo · T. Wu · X. Li
Beijing Key Laboratory of Restoration of Damaged Ocular Nerve, Peking University Third Hospital, Beijing, China

S. Sun
Peking University Health Science Center, Beijing, China

Background

Cataract remains the leading cause of vision loss [1]. Phacoemulsification (PHACO) combined with Intraocular lens (IOL) implantation is the most commonly used procedure [2]. With the continuous development of IOL design and calculation formula, the surgery aims to achieve optimized visual quality beyond visual acuity improvement [3]. Therefore, in recent years, precise refractive status prediction following surgery has aroused public attention. The prediction of the postoperative refraction depends on the accuracy of the biometry and IOL calculation formulas [4]. Postoperative anterior chamber depth (ACD) or effective lens position (ELP) prediction is a critical element in postoperative refractive accuracy [5–7]. False forward or backward prediction of ELP causes a myopic or hyperopic shift. The previous literature reported that about 40% of postoperative refractive errors are caused by inaccurate predictions of postoperative ACD or ELP [8–10].

Under physiological conditions, anterior chamber depth (ACD) depends on lens thickness and its relationship regarding the anterior segment structures [11–16]. Studies have confirmed that cataract surgery and IOL implantation deepen the anterior chamber [11–19]. In prior research, the ACD was only measured and predicted along the axis in cataract surgery. However, due to factors including the difference in the corneal and iris biomechanics at different regions and the specific IOL design on paraxial and peripheral areas, the changes of ACD at different locations on the iris plane after the surgery might be uneven [20–22]. Thus, predicting the axial or central ELP only facilitates the accurate prediction of postoperative refractive error (lower-order wavefront aberration), and the disparity in the ACD changes at different areas has not been considered before which might cause high-order wavefront aberration.

Additionally, the visual quality after implantation of most commercially available IOLs depends on the pupil size because of the inconsistency in the refraction for paraxial and peripheral light wave [23–25]. The aspherical and surface microstructure designs aim to solve problems [22, 26]. However, these designs only consider the effect of cornea and IOL on the entering light, and the refraction induced by ACD topographic changes has not been considered. Thus, studies exploring ACD topographic changes are required that might improve the topographic ELP prediction and IOL design. Here, the present research applied Pentacam to measure the ACD at different regions before and after PHACO combined with IOL implantation to obtain topographic changes of ACD and further explore its related factors.

Methods

Participants

This present study was a retrospective cohort research. The research protocol was approved by the Ethics Committee of the Peking University Third Hospital Eye Center, and the research was conducted following the principles of the Declaration of Helsinki.

The research enrolled consecutive patients with age-related cataract undergoing standard PHACO with IOL implantation surgery between July and December 2019 from Peking University Third Hospital. Exclusion criteria included patients with (1) diseases that had a significant impact on ACD, including congenital iris and anterior chamber angle (ACA) abnormality and so on; (2) a history of ocular trauma that has an impact on the structure of the anterior segment, including angle recession, dialysis of the ciliary body, and so on; (3) a history of internal ocular surgery; and (4) intraoperative or severe postoperative complications including posterior capsule tear; zonular dialysis; IOL tilting, subluxation or dislocation; prolonged postoperative inflammation and so on.

Preoperative and postoperative evaluation

Each participant was subjected to comprehensive preoperative ocular evaluations, including history-taking with specific attention to the disease and trauma that might impact the anatomy of the anterior segment, visual acuity, intraocular pressure with noncontact tonometry, routine fundus examination, slit-lamp biomicroscopy to assess the cataract and anterior segment structure, automated biometry with IOL master 700 (Carl Zeiss Meditec AG, Jena, German), Pentacam (OCULUS, German). The preoperative axial length (AL), keratometry (K) and corneal diameter (white to white, WTW) were obtained from IOL Master 700 examination.

The Pentacam was performed to evaluate ACDs before and approximately four weeks after the surgery. The subjects were instructed to remain stationary, keeping both eyes open. The subjects were dark adapted before the measurement. Images were captured, while subjects fixated on the internal fixation target. The Pentacam took 25 images per measurement from various orientations. Re-measurement was performed if the image quality mark was red or yellow for the anterior and posterior cornea. The display mode of "One Large Color Map" with the data of ACD was shown, and the data at a distance to the corneal apex (DCA) of 2 mm (8 points), 4 mm (12 points), 6 mm (16 points) and 8 mm (20 points) were recorded. Images were discarded if the quality tests of the anterior and posterior cornea surface showed abnormalities, including problems on the data within the analyzed area, segment loss, alignment or eye movements following re-measurements. Images with obvious focal ACD abnormalities such as focal depression or aberrant elevation were nullified. Moreover, images with apparent changes in the relative location between the corneal apex and pupil center before and after the surgery were also excluded.

Surgical technique

All operations were performed by the same right-handed surgeon using standard PHACO technique sitting superior to the patients' heads. After topical anesthesia was administered, a 3.0-mm clear corneal incision was created with the right hand at 11'O clock. Following filling with the viscous agent in the anterior chamber, a continuous curvilinear capsulorhexis with a diameter of approximately 5.0 mm was established. And hydrodissection and hydrodelamination were performed with a 27-gauge cannula. The cataractous lens was removed with coaxial PHACO with Constellation Vision System (Alcon Laboratory Inc., USA). The cortical remnants were removed with an automated irrigation/aspiration, and the posterior capsule was polished. A foldable aspherical IOL was then implanted in the capsular bag.

Statistical analysis and piloting

The data were analyzed using SPSS software (version 24.0, SPSS, Inc.). The continuous variables were presented as mean and standard deviation (SD), and the number and percentage were shown for categorical variables. The absolute changes of ACD (AACD) were calculated as postoperative ACD subtracted by preoperative ACD at the same location, and the relative changes of ACD (RACD) were defined as the ratio of postoperative ACD to preoperative ACD. The cornea was quartered with vertical and horizontal meridians on the topography. The temporal region was defined as the anterior chamber on the temporal side of the vertical meridian and the same to the nasal, and the superior region was defined as the site above the horizontal meridian, the same as inferior region. A multiple linear model with stepwise regression was performed to demonstrate the impact of age, gender, DCA, temporal–nasal side, superior–inferior side, AL, average K and WTW on AACD and RACD, and full-factor analysis of variance considering the interaction among factors was used to compare the difference of AACD and RACD at different locations adjusted for the age and DCA as co-variants. According to the DCA (2 mm, 4 mm, more than 6 mm), subgroup analysis was performed to manifest the impact of the above factors on paraxial and peripheral AACD and RACD. A *P*-value of less than 0.05 was considered statistically significant.

The plotting of the three-dimensional ACD topographic changes was performed with Matlab R2018a (MathWorks, Natick, MA, USA). Scatter3(X, Y, Z) plotted the mean AACD values and mean RACD representatively as heights specified by Z above the x–y plane defined by different iris plane regions. Error bars were added to the scattered spots using plot3 (X, Y, Z'), which plotted a set of coordinates connected by line segments in three-dimensional space with Z' standing for mean ± SD. Surf (X, Y, Z) plotted a surface covering the spots of mean values of AACD and RACD representatively above a grid in the x–y plane, and we chose the biharmonic spline interpolation method (MATLAB® four griddata method). The color of the surface varied according to the heights.

Results

Demographic parameters

Data from 78 eyes of 61 patients (51 eyes from women [65.4%] and 27 eyes from men [34.6%]) were elicited for analysis, and the mean age was 71.1 ± 9.3 years

(range 52-90 years). The baseline characteristics of the study are summarized in Table 1.

AACD and RACD topographic contour

Figure 1A, B shows the three-dimensional surface of AACD and RACD topography plotting mean value and error bar, and Fig. 1C, D demonstrates the contour. The AACD generally declined from central to the peripheral in all directions, indicating the disparity of ACD changes at different locations on the iris plane. The plotting of the RACD topographic contour was similar to that of AACD, but the difference in the heights from central to peripheral specified by Z-axis was less evident than AACD. Furthermore, the shape of AACD and RACD topography was not centrosymmetric or axisymmetric along the X- and Y-axis.

Influential factors of AACD and RACD

The results from multiple linear regression (AACD: $R^2 = 0.381$, $p < 0.001$; RACD: $R^2 = 0.268$, $p < 0.001$) are summarized in Table 2. Age, DCA, gender, AL, average K and temporal–nasal location on the iris plane significantly affected the AACD. The model revealed a positive correlation between the age ($\beta = 0.282$, $p < 0.001$) and average K ($\beta = 0.073$, $p < 0.001$) of patients and the AACD, and a negative correlation between the DCA (β = -0.436, $p < 0.001$), AL ($\beta = -0.165$, $p < 0.001$) and the AACD. RACD was also significantly influenced by age, DCA, gender, AL, average K and WTW. Multiple linear regression revealed that RACD was also positively correlated with age ($\beta = 0.311$, $p < 0.001$) and average K ($\beta = 0.081$, $p < 0.001$) and negatively correlated with the DCA ($\beta = -0.121$, $p < 0.001$), AL ($\beta = -0.23$, $p < 0.001$) and WTW ($\beta = -0.106$, $p < 0.001$).

The result of the full-factor analysis of variance is summarized in Table 3. The AACD was significantly greater in female than in male ($p < 0.001$), and the AACD at the temporal region was significantly larger than that at the nasal region ($p < 0.001$), and significantly larger AACD was demonstrated at the inferior region compared with the superior region ($p < 0.001$). The RACD was also significantly greater in females than in males ($p < 0.001$), and no significant difference of RACD was found between temporal and nasal or superior and inferior location.

Subgroup analysis according to DCA for influential factors of AACD and RACD

The results of the subgroup analysis are summarized in Table 4 and Table 5. We found an increase in the AACD with age in each of the three subgroups ($p < 0.001$). The AACD adjusted by age was significantly greater in females than in males at the DCA of 2 mm ($p = 0.003$), 4 mm ($p < 0.001$) and more than 6 mm ($p = 0.006$). At the DCA of 2 mm, the AACD was significantly greater in the inferior region than at the superior region ($p < 0.001$). At the DCA of more than 6 mm, the AACD was significantly greater at the temporal region than at the nasal region ($p = 0.002$) and greater at the inferior region than at the superior region ($p = 0.034$). The RACD showed a similar trend of increase with age at the DCA of 2 mm, 4 mm and more than 6 mm ($p < 0.001$). And the RACD adjusted by age was also significantly greater in female than in male in each of the three subgroups ($p < 0.001$). As for location, the RACD was significantly greater in the inferior region than at the superior region only at the DCA of 2 mm ($p = 0.001$).

Table 1 Demographics, preoperative ocular parameters and surgical parameters (78 eyes of 61 subjects)

Parameter	Mean ± SD	Range
Age (yrs)	71.17 ± 9.32	52–90
Male (subjects), n (%)	20 (32.79)	NA
Male (eye), n (%)	27 (34.62)	NA
Corneal astigmatism (D)	0.45 ± 0.79	− 1.98 ~ 2.63
Predicted refraction (D)	− 0.21 ± 0.68	− 3.22 ~ 0.23
AL (mm)	23.69 ± 1.91	21.29 ~ 35.74
K1 (Flat, D)	44.16 ± 1.50	39.00 ~ 47.87
K2 (Steep, D)	45.02 ± 1.35	42.14 ~ 48.42
WTW (mm)	11.68 ± 0.46	10.50 ~ 12.90
ACV (mm^3)	119.90 ± 42.82	49.00 ~ 277.00
ACD (mm)	2.55 ± 0.44	1.50 ~ 3.55

AL, axial length; *K*, keratometry; *ACD*, anterior chamber depth; *WTW*, white-to-white depth; *ACV*, anterior chamber volume; *NA*, not available

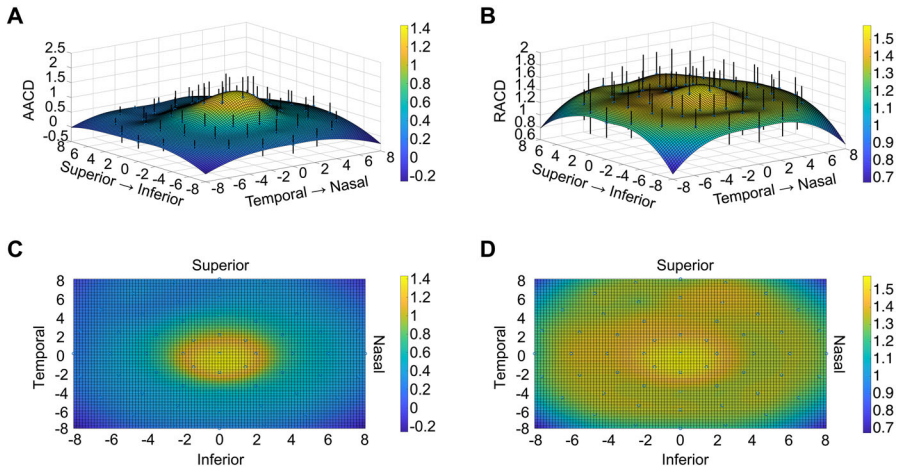

Fig. 1 AACD and RACD topographic contour. **A** and **B**: three-dimensional surface of AACD and RACD topographic changes plotting mean value and error bar; **C** and **D**: the topographic contour of AACD and RACD

Table 2 Multiple linear regression of the influential factors

	Factors	Unstandardized coefficients	Standard deviation	Standardized coefficients	*P*
AACD	DCA	− 0.124	0.004	− 0.436	< 0.001
	Age	0.018	0.001	0.282	< 0.001
	AL	− 0.048	0.004	− 0.165	< 0.001
	Average K	0.03	0.006	0.073	< 0.001
	TN	− 0.042	0.012	− 0.053	< 0.001
	Gender	0.036	0.018	0.029	0.05
RACD	Age	0.012	0.001	0.311	< 0.001
	AL	− 0.04	0.003	− 0.23	< 0.001
	DCA	− 0.021	0.003	− 0.121	< 0.001
	WTW	− 0.081	0.013	− 0.106	< 0.001
	Gender	0.115	0.012	0.160	< 0.001
	Average K	0.02	0.004	0.081	< 0.001

AACD, absolute anterior chamber depth; *RACD*, relative anterior chamber depth; *DCA*, distance to corneal apex; *TN*, temporal–nasal; *SI*, superior–inferior; *AL*, axial length; *K*, keratometry; *WTW*, white to white

Discussion

The present research innovatively investigated the ACD topographic changes following cataract surgery with IOL implantation. We calculated two indexes: AACD and RACD, as they have different but rather essential implications. AACD stands for the absolute change of ACD following the surgery, which is instructive to predict refractive state and IOL selection [8]. Meanwhile, due to the inherent differences in ACD at different locations, simply calculating the change in absolute value does not fully reflect the degree of the changes. Therefore, the relative value, RACD, was also calculated to facilitate analyzing the effect of different factors on the change of ACD.

Analyzed either with the full dataset or at different DCA, both AACD and RACD significantly increased with age, which means that older subjects tend to have more remarkable changes in ACD at both paraxial and peripheral regions after cataract surgery. The result was consistent with previous research that the central ACD changes were positively related to age [27]. It has been acknowledged that central ACD changes negatively correlate with preoperative ACD and have a positive correlation with lens thickness (LT) [8].We know that age-related cataract tends to be more severe

Table 3 Full-factor analysis of variance of gender, temporal–nasal, and superior–inferior adjusted for age and DCA

	Factors	Mean (SD)	N	*P*
AACD	Male	0.64 (0.53)	1060	< 0.001
	Female	0.63 (0.58)	2200	
	Temporal	0.61 (0.54)	1426	< 0.001
	Nasal	0.58 (0.54)	1273	
	Superior	0.58 (0.52)	1246	< 0.001
	Inferior	0.62 (0.57)	1401	
RACD	Male	1.35 (0.27)	1060	< 0.001
	Female	1.39 (0.37)	2200	
	Temporal	1.36 (0.32)	1426	0.115
	Nasal	1.38 (0.35)	1273	
	Superior	1.38 (0.36)	1246	0.862
	Inferior	1.36 (0.32)	1401	

AACD, absolute anterior chamber depth; *RACD*, relative anterior chamber depth; *DCA*, distance to corneal apex; *SD*, standard deviation; *SE*, standard error; *N*, number of points

Table 5 *P*-value of full-factor analysis of variance in gender, temporal–nasal, and superior–inferior adjusted for age in subgroup analysis according to DCA

DCA (mm)		2	4	6–8
AACD	Gender	0.003	< 0.001	0.006
	Age	< 0.001	< 0.001	< 0.001
	TN	0.374	0.135	0.002
	SI	< 0.001	0.548	0.034
RACD	Gender	< 0.001	< 0.001	< 0.001
	Age	< 0.001	< 0.001	< 0.001
	TN	0.619	0.021	0.410
	SI	0.001	0.194	0.161

AACD, absolute anterior chamber depth; *RACD*, relative anterior chamber depth; *DCA*, distance to corneal apex; *TN*, temporal–nasal; *SI*, superior–inferior

in older people, and the lens grows thicker with age, which might push the iris forward and result in the shallow AC [28–30]. So replacing the instinct lens with a thinner IOL could significantly increase ACD at all of the AC regions. Thus, following IOL implantation, the age-related greater ACD changes might be associated with the greater disparity between LT and IOL thickness.

DCA is another factor that significantly affected AACD and RACD, both of which were greater in the central than peripheral region. Our results also showed that the absolute value of the standardized regression coefficient for DCA in the AACD model is larger than that in the RACD model. The regression coefficient's difference suggested that the effect of DCA on ACD topography was partially associated with preoperative ACD distribution. The maximal changes in the central ACD might be attributed to the greatest preoperative ACD at the paraxial region. Since RACD was still significantly affected by DCA, there should be other mechanisms. The fibers in the central corneal stromal layer are organized more regularly than the peripheral fibers, which induces disparity in the mechanical

Table 4 Descriptive results of subgroup analysis according to DCA

DCA (mm)		2		4		6 ~ 8	
		Mean (SD)	*N*	Mean (SD)	*N*	Mean (SD)	*N*
AACD (mm)	Male	1.05 (0.65)	216	0.61 (0.40)	324	0.44 (0.39)	493
	Female	1.15 (0.63)	432	0.61 (0.44)	648	0.40 (0.46)	1066
	Temporal	1.13 (0.61)	243	0.63 (0.43)	405	0.44 (0.48)	778
	Nasal	1.08 (0.66)	243	0.59 (0.42)	405	0.37 (0.41)	625
	Superior	0.99 (0.57)	243	0.60 (0.44)	405	0.39 (0.46)	598
	Inferior	1.25 (0.68)	243	0.62 (0.44)	405	0.42 (0.43)	753
RACD (%)	Male	1.43 (0.28)	216	1.33 (0.23)	324	1.31 (0.28)	493
	Female	1.50 (0.31)	432	1.37 (0.32)	648	1.35 (0.40)	1066
	Temporal	1.47 (0.29)	243	1.34 (0.27)	405	1.33 (0.35)	778
	Nasal	1.48 (0.32)	243	1.38 (0.32)	405	1.34 (0.37)	625
	Superior	1.44 (0.28)	243	1.37 (0.31)	405	1.32 (0.33)	598
	Inferior	1.52 (0.30)	243	1.35 (0.29)	405	1.34 (0.37)	753

AACD, absolute anterior chamber depth; *RACD*, relative anterior chamber depth; *DCA*, distance to corneal apex; *SD*, standard deviation; *N*, number of points

strength [20, 31]. Consequently, the central cornea might be more likely to deform. Moreover, the difference between the central and peripheral iris changes might also count. The expanded cataractous lens exerted greater propulsion on the central iris. Thus, the central iris might descend more following the surgery so that the central ACD possesses more tremendous changes [27, 31].

AACD was significantly greater at the temporal region than at the nasal region, and the significant difference was only detected peripherally. ACA, trabecular-iris angle (TIA), trabecular-iris surface area (TISA) and angle opening distance (AOD) have been previously analyzed, and these studies mainly demonstrated that the widening of the anterior chamber angle was greater at the nasal than the temporal quadrant. Nolan revealed that the postoperative AOD_{500} and $TISA_{750}$ increased by about 80% at the nasal quadrant and about 55% at the temporal quadrant [32]. Kim showed similar results that the AOD and TISA increased by about 85% at the nasal quadrant and 55% at the temporal quadrant in patients with open-angle glaucoma [33]. Pereira also reported the ACA to widen 1.26 times temporally and 1.53 times nasally [13]. The inconsistency in the result might be attributed to the examination methods and distance to the apex. The established studies mainly applied anterior segment optical coherence tomography (AS-OCT) or ultrasound to evaluate ACA, and the present research utilized Pentacam to measure the paraxial and peripheral ACD. Previous research showed that results of ACA measured with AS-OCT and Pentacam are different, and nasal ACA measured with Pentacam is smaller than that with AS-OCT for normal angle [34]. That may account for the smaller change in nasal ACD postoperatively. Additionally, the present research only measured the ACD up to 8 mm to the corneal apex, different from the ACA measured at the limbus. Future research could consider the anatomic and biomechanics differences between the nasal and temporal ACA to further demonstrate the disparity in the influence of cataract surgery on ACA.

Superior–inferior location significantly affects both AACD and RACD, both of which were greater at the inferior region on the whole. At the DCA of more than 6 mm, the result of AACD was similarly affected, but not RACD. Previous research revealed less increase in ACA superiorly compared to elsewhere in the AC [35]. In another study, the ACA has been reported to widen 1.36 times superiorly and 1.52 times inferiorly [13]. During the surgery, the main incision is conducted on the superior region of the cornea. Thus, the flow direction during emulsification and irrigation/aspiration is often downward, and the flow is faster in the inferior region [36]. Additionally, during the tissue remodeling process of the incision, type III collagen was produced, and the stromal cells might be transformed into myofibroblasts, which have a contraction function [37], probably making the changes of ACD at the superior region smaller than that in the inferior region.

This present study investigated the topographic changes of ACD after cataract surgery and has significant clinical implications. Firstly, the depiction of the ACD topographic map changes facilitates the summary and establishment of mathematical formulas or models to predict the changes of the entire ELP postoperatively in the future. The central ACD changes are in analogy with the translation of an optical element, and uneven changes in the ACD topography involve deformation of the element that involves higher-order aberrations. Thereby, surgeons could better achieve optimized visual quality following cataract surgeries. Secondly, considering the postoperative ACD topographic changes could further improve IOL design. To achieve pupil independence in IOL design, the difference in paraxial and peripheral ACD changes must be considered apart from the influence of IOL on paraxial and peripheral light waves. The surface microstructure on the IOL optic zone should be designed to compensate for the disparity in ACD changes centrally and peripherally, which reduces higher-order aberrations.

The limitation of our study involves that the population of the included patients was relatively small; the patients have been followed for only one month, and they are still under regular follow-ups for further research; also, quite a few data at the DCA of 8 mm failed to be recorded by Pentacam due to the limitation of the machine. Moreover, postoperative ACD changes could be affected by multiple factors, and potentially influential factors including intraocular pressure and axial length should be considered in future research. Further mathematical models for simulating the effect of ACD changes at different locations on the wavefront aberrations ought to be developed.

In conclusion, we successfully used Pentacam to reliably and reproducibly measure the ACD at different regions before and after PHACO combined with IOL implantation and depicted the three-dimensional ACD topographic changes. The research found that both AACD and RACD were positively correlated with age and negatively correlated with the DCA. Moreover, AACD and RACD were also significantly influenced by gender and quadrant location. The research provides the basis for further improving postoperative refraction prediction accuracy and IOL design independent of the pupil size.

Authors contributions YW, SS and XL contributed to the conception and design of the research. SW, YG and TW are responsible for data collection and follow-up. YW and SS performed the data analysis and wrote the initial draft. All of the authors contributed to the revision of the draft and are responsible for the final approval.

Funding This work was supported by the grant from Chinese Capital's Funds for Health Improvement and Research (Grant number: CFH2018-2–4093) and the National Science and Technology Major Project (Grant number: 2018ZX10101004). The sponsor or funding organization had no role in the design or conduct of this research.

Data availability The datasets generated during and analyzed during the current study are available from the corresponding author on reasonable request following publication.

Declarations

Conflict of interests The authors declare that they have no competing interests.

Ethics approval The research protocol was approved by the Ethics Committee of the Peking University Third Hospital Eye Center.

Consent to participate This research study was conducted retrospectively from data obtained for clinical purposes. Exemption of informed consent was approved by the ethics committee.

References

1. Flaxman SR, Bourne RRA, Resnikoff S, Ackland P, Braithwaite T, Cicinelli MV, Das A, Jonas JB, Keeffe J, Kempen JH, Leasher J, Limburg H, Naidoo K, Pesudovs K, Silvester A, Stevens GA, Tahhan N, Wong TY, Taylor HR (2017) Global causes of blindness and distance vision impairment 1990–2020: a systematic review and meta-analysis. Lancet Glob Health 5(12):e1221–e1234. https://doi.org/10.1016/s2214-109x(17)30393-5
2. Asbell PA, Dualan I, Mindel J, Brocks D, Ahmad M, Epstein S (2005) Age-related cataract. Lancet (London, England) 365(9459):599–609. https://doi.org/10.1016/s0140-6736(05)17911-2
3. Zaidi FH, Corbett MC, Burton BJ, Bloom PA (2007) Raising the benchmark for the 21st century–the 1000 cataract operations audit and survey: outcomes, consultant-supervised training and sourcing NHS choice. Br J Ophthalmol 91(6):731–736. https://doi.org/10.1136/bjo.2006.104216
4. Olsen T (2006) Prediction of the effective postoperative (intraocular lens) anterior chamber depth. J Cataract Refract Surg 32(3):419–424. https://doi.org/10.1016/j.jcrs.2005.12.139
5. Goto S, Maeda N, Koh S, Ohnuma K, Hayashi K, Iehisa I, Noda T, Nishida K (2016) Prediction of postoperative intraocular lens position with angle-to-angle depth using anterior segment optical coherence tomography. Ophthalmology 123(12):2474–2480. https://doi.org/10.1016/j.ophtha.2016.09.005
6. Tamaoki A, Kojima T, Tanaka Y, Hasegawa A, Kaga T, Ichikawa K, Tanaka K (2019) Prediction of effective lens position using multiobjective evolutionary algorithm. Trans Vis Sci Technol 8(3):64. https://doi.org/10.1167/tvst.8.3.64
7. Jin H, Rabsilber T, Ehmer A, Borkenstein AF, Limberger IJ, Guo H, Auffarth GU (2009) Comparison of ray-tracing method and thin-lens formula in intraocular lens power calculations. J Cataract Refract Surg 35(4):650–662. https://doi.org/10.1016/j.jcrs.2008.12.015
8. Olsen T (2007) Calculation of intraocular lens power: a review. Acta Ophthalmol Scand 85(5):472–485. https://doi.org/10.1111/j.1600-0420.2007.00879.x
9. Sahin A, Hamrah P (2012) Clinically relevant biometry. Curr Opin Ophthalmol 23(1):47–53. https://doi.org/10.1097/ICU.0b013e32834cd63e
10. Norrby S (2008) Sources of error in intraocular lens power calculation. J Cataract Refract Surg 34(3):368–376. https://doi.org/10.1016/j.jcrs.2007.10.031
11. Steuhl KP, Marahrens P, Frohn C, Frohn A (1992) Intraocular pressure and anterior chamber depth before and after extracapsular cataract extraction with posterior chamber lens implantation. Ophthalmic Surg 23(4):233–237
12. Simsek A, Ciftci S (2012) Evaluation of ultrasonic biomicroscopy results in anterior eye segment before and after cataract surgery. Clin Ophthalmol 6:1931–1934. https://doi.org/10.2147/opth.s37614
13. Pereira FA, Cronemberger S (2003) Ultrasound biomicroscopic study of anterior segment changes after phacoemulsification and foldable intraocular lens implantation. Ophthalmology 110(9):1799–1806. https://doi.org/10.1016/s0161-6420(03)00623-7
14. Hayashi K, Hayashi H, Nakao F, Hayashi F (2000) Changes in anterior chamber angle width and depth after intraocular lens implantation in eyes with glaucoma. Ophthalmology 107(4):698–703. https://doi.org/10.1016/s0161-6420(00)00007-5
15. Dooley I, Charalampidou S, Malik A, Loughman J, Molloy L, Beatty S (2010) Changes in intraocular pressure and

anterior segment morphometry after uneventful phacoemulsification cataract surgery. Eye 24(4):519–526. https://doi.org/10.1038/eye.2009.339
16. Cho YK (2008) Early intraocular pressure and anterior chamber depth changes after phacoemulsification and intraocular lens implantation in nonglaucomatous eyes Comparison of groups stratified by axial length. J Cataract Refractive Surg 34(7):1104–1109. https://doi.org/10.1016/j.jcrs.2008.03.023
17. Tarongoy P, Ho CL, Walton DS (2009) Angle-closure glaucoma: the role of the lens in the pathogenesis, prevention, and treatment. Surv Ophthalmol 54(2):211–225. https://doi.org/10.1016/j.survophthal.2008.12.002
18. Gunning FP, Greve EL (1991) Uncontrolled primary angle closure glaucoma: results of early intercapsular cataract extraction and posterior chamber lens implantation. Int Ophthalmol 15(4):237–247. https://doi.org/10.1007/bf00171026
19. Gunning FP, Greve EL (1998) Lens extraction for uncontrolled angle-closure glaucoma: long-term follow-up. J Cataract Refract Surg 24(10):1347–1356. https://doi.org/10.1016/s0886-3350(98)80227-7
20. Ma J, Wang Y, Wei P, Jhanji V (2018) Biomechanics and structure of the cornea: implications and association with corneal disorders. Surv Ophthalmol 63(6):851–861. https://doi.org/10.1016/j.survophthal.2018.05.004
21. Pant AD, Dorairaj SK, Amini R (2018) Appropriate Objective Functions for Quantifying Iris Mechanical Properties Using Inverse Finite Element Modeling. J Biomech Eng. https://doi.org/10.1115/1.4039679
22. Dick HB (2009) Recent developments in aspheric intraocular lenses. Curr Opin Ophthalmol 20(1):25–32. https://doi.org/10.1097/ICU.0b013e32831b8bb3
23. Petermeier K, Frank C, Gekeler F, Spitzer MS, Messias A, Szurman P (2011) Influence of the pupil size on visual quality and spherical aberration after implantation of the Tecnis 1-piece intraocular lens. Br J Ophthalmol 95(1):42–45. https://doi.org/10.1136/bjo.2009.169680
24. Pandita D, Raj SM, Vasavada VA, Vasavada VA, Kazi NS, Vasavada AR (2007) Contrast sensitivity and glare disability after implantation of AcrySof IQ Natural aspherical intraocular lens: prospective randomized masked clinical trial. J Cataract Refract Surg 33(4):603–610. https://doi.org/10.1016/j.jcrs.2007.01.009
25. Salati C, Salvetat ML, Zeppieri M, Brusini P (2007) Pupil size influence on the intraocular performance of the multifocal AMO-Array intraocular lens in elderly patients. Eur J Ophthalmol 17(4):571–578. https://doi.org/10.1177/112067210701700415
26. Mester U, Dillinger P, Anterist N (2003) Impact of a modified optic design on visual function: clinical comparative study. J Cataract Refract Surg 29(4):652–660. https://doi.org/10.1016/s0886-3350(02)01983-1
27. Fallah Tafti MR, Abdollah Beiki H, Mohammadi SF, Latifi G, Ashrafi E, Fallah Tafti Z (2017) Anterior chamber depth change following cataract surgery in pseudoexfoliation syndrome; a preliminary study. J Ophthalmic Vis Res 12(2):165–169. https://doi.org/10.4103/jovr.jovr_81_15
28. Klein BE, Klein R, Moss SE (2000) Lens thickness and five-year cumulative incidence of cataracts: The Beaver Dam Eye Study. Ophthalmic Epidemiol 7(4):243–248. https://doi.org/10.1076/opep.7.4.243.4176
29. Dubbelman M, van der Heijde GL, Weeber HA (2001) The thickness of the aging human lens obtained from corrected Scheimpflug images. Optometry Vis Sci 78(6):411–416. https://doi.org/10.1097/00006324-200106000-00013
30. Kim M, Park KH, Kim TW, Kim DM (2011) Changes in anterior chamber configuration after cataract surgery as measured by anterior segment optical coherence tomography. Korean J Ophthalmol 25(2):77–83. https://doi.org/10.3341/kjo.2011.25.2.77
31. Eghrari AO, Riazuddin SA, Gottsch JD (2015) Overview of the cornea: structure, function, and development. Prog Mol Biol Transl Sci 134:7–23. https://doi.org/10.1016/bs.pmbts.2015.04.001
32. Nolan WP, See JL, Aung T, Friedman DS, Chan YH, Smith SD, Zheng C, Huang D, Foster PJ, Chew PT (2008) Changes in angle configuration after phacoemulsification measured by anterior segment optical coherence tomography. J Glaucoma 17(6):455–459. https://doi.org/10.1097/IJG.0b013e3181650f31
33. Kim M, Park KH, Kim TW, Kim DM (2012) Anterior chamber configuration changes after cataract surgery in eyes with glaucoma. Korean J Ophthalmol 26(2):97–103. https://doi.org/10.3341/kjo.2012.26.2.97
34. Yi JH, Hong S, Seong GJ, Kang SY, Ma KT, Kim CY (2008) Anterior chamber measurements by pentacam and AS-OCT in eyes with normal open angles. Korean J Ophthalmol 22(4):242–245. https://doi.org/10.3341/kjo.2008.22.4.242
35. Lee H, Zukaite I, Juniat V, Dimitry ME, Lewis A, Nanavaty MA (2019) Changes in symmetry of anterior chamber following routine cataract surgery in non-glaucomatous eyes. Eye and Vis 6:19. https://doi.org/10.1186/s40662-019-0144-3
36. Garbee DD (1997) Phacoemulsification procedures performed with topical anesthesia. AORN J 66(2):260–262. https://doi.org/10.1016/s0001-2092(06)62794-4
37. Tanaka S, Saika S, Ohmi S, Miyamoto T, Ishida I, Okada Y, Yamanaka O, Ohnishi Y, Ooshima A (2002) Cellular fibronectin, but not collagens, disappears in the central posterior capsules during healing after lens extraction and IOL implantation in rabbits. Jpn J Ophthalmol 46(2):147–152. https://doi.org/10.1016/s0021-5155(01)00503-2